International Journal of Advancements in Technology

Vivekanandan, Int J Adv Technol 2018, 9:1
DOI: 10.4172/0976-4860.1000199

Research Article Open Access

Comparison of Artificial Neural Network and Regression Approaches for Evaluation of Hydrodynamic Performance of Quarter Circular Break Water

N Vivekanandan*

Central Water and Power Research Station, Pune, Maharashtra, India

Abstract

Quarter-circular Break Water (QBW) is a modified semi-circular breakwater, which are similar to caisson consists of a quarter circular surface facing incident waves, with horizontal bottom and a rear vertical wall and are generally placed on a rubble mound foundation. QBW may be constructed as emerged with and without perforations that may be one side or on either sides. By these perforations, the energy is dissipated owing to the formation of eddies and turbulence is created inside the hollow chamber. In this paper, the data collected from the experimental work carried out at National Institute of Technology, Surathkal is analysed by plotting the non-dimensional graphs of reflection coefficient, reflected wave height and incident wave height for various values of wave steepness. These values are used for prediction of QBW adopting Artificial Neural Network (ANN) and Regression (REG) approaches. In ANN, Multi layer Perceptron (MLP) and Radial Basis Function networks are considered for training the network data. Goodness-of-Fit (GoF) test *viz.*, Kolmogorov-Smirnov test statistic and Model Performance Analysis (MPA) *viz.*, correlation coefficient, mean absolute error and model efficiency are applied for checking the adequacy of ANN and REG approaches to the observed data. The results of GoF test and MPA indicates the MLP is better suited for evaluation of hydrodynamic performance of QBW.

Keywords: Auto-regression; Correlation coefficient; Kolmogorov-Smirnov test; Model efficiency; Multi layer perceptron; Radial basis function; Mean absolute error

Introduction

Breakwater is a structure generally, used in coastal protection works and also for creating tranquillity in basin in harbours. Over the year's breakwater were of rubble mound weighing in tons. In the latter part of 19th century innovative structures like tetrapods, tripods and other interlocking blocks are also evolved. Considering the huge quantity of rock material required, in the beginning of 21st century caisson type of breakwater were thought off. One such breakwater is Quarter-circular Break Water (QBW), a new-type breakwater first proposed by Xie et al [1] on the basis of Semi-circular Break Water (SBW). The QBW is usually placed on rubble mound foundation and its superstructure consists of a quarter circular surface facing sea sides, a horizontal bottom and a rear vertical wall. The QBW structure is hollow, hence, the weight and materials required are less and it is more suitable where the foundation is relatively weak. The QBW is a prefabricated caisson, which can be properly designed for handling stresses and can be transported and placed with more precision at the desired location. Depending upon the purpose the QBW may be fabricated as emerged type structure, with and without perforation to dissipate the incident wave energy.

Literature Review

Jiang et al [2] studied the performance of QBW by comparing the hydraulic performances of QBW and SBW under similar hydraulic conditions. They conducted 2-dimensional (2D) vertical wave numerical model and physical model studies, and found that wave reflection of both QBW and SBW are closer to each other. They stated that the wave reflection coefficient (K_r) remains almost same with values less than 1.0 even when free board (h_c) value becomes 2 to 3 times incident wave height (H_i) for both types of breakwaters. During wave overtopping in submerged condition, they found high flow velocity and vortexes near the rear walls of QBW, which may be due to top sharp corner and sudden expansion of flow around QBW. They described that the flow fields in front of both QBW and SBW are similar in both in submerged as well as emerged conditions and this explains the closeness of reflection coefficient (K_r) values for both breakwaters.

Shi et al [3] studied the hydrodynamic performance of QBW under both regular and irregular wave conditions. Regular waves were generated by reciprocating wave paddle at constant speed whereas irregular waves were generated by frequency spectrum simulation with target spectrum of JONSWAP type. For analysing the wave reflection, two types of wave reflection coefficients were described by Shao [4] viz., (i) K_r that describes the whole effect of wave reflection by breakwater and (ii) Circular-surface reflection coefficient (K_{rc}) that describes the reflective effect by circular surface on the adjacent flow field in front of the breakwater. He found that at the same relative freeboard height (h_c/H_i), the value of K_r was higher than K_{rc} that indicates the entire reflective effect of QBW is stronger than that by circular surface on the adjacent flow field. To estimate the energy dissipation as the wave passes over the breakwater wave energy loss parameter (K_{Eloss}) was described. K_{Eloss} is the ratio of dissipated wave energy to the original gross wave energy within the process of wave structure interaction. Based on the results obtained from the study, it was found that the loss of wave energy for emerged breakwater is larger than that for submerged breakwater.

Hegde and Ravikiran [5] conducted experiments on physical model of QBW in 2D wave flumes to evaluate the reflection characteristics of QBW of different radii in different submergence conditions. The models were made of galvanized iron sheets and coated with cement slurry to simulate concrete surface. For finding the variation of K_r different graphs were plotted with the incident wave steepness (H_i/gT^2) (where, g is the gravitation and T is the wave period) for various submergence ratios (d/h_c) and different ranges of (R/H_i) (where, d is the depth of water and R is the breakwater radius). For all values of d/h_c and

***Corresponding author:** Shri. N Vivekanandan, Scientist-B, Central Water and Power Research Station, Pune, Maharashtra, India, E-mail: vivek.cwprs@gmail.com

Received: January 29, 2018; **Accepted:** February 19, 2018; **Published:** February 26, 2018

Citation: Vivekanandan N (2018) Comparison of Artificial Neural Network and Regression Approaches for Evaluation of Hydrodynamic Performance of Quarter Circular Break Water. Int J Adv Technol 9: 199. doi:10.4172/0976-4860.1000199

R/H_i, they found that K_r increases logarithmically (best-fit) as incident wave steepness increases. The study revealed that whatever may be the depth, caisson radius, height of structure crest (from sea bed) steeper the waves the more will be the reflection from breakwater. Hafeeda [6] conducted experiments in a 2D monochromatic wave flume on a seaside perforated QBW model. He analyzed the experimental data by plotting the non-dimensional graphs of K_r (i.e., H_r/H_i) (where, H_r is the reflected wave height) for various values of R/H_i. He observed that the value of K_r increased with increase in wave steepness and when the free board (h_c) increased then the value of K_r also increased. He found that when height of the structure (h_s) increases, smaller height of the QBW portion of the caisson is exposed to waves, which is effect of the curvature is less pronounced that tend to lesser dissipation and more reflection.

Binumol et al [7] conducted physical model studies of QBW with three different radii and S/D (spacing to diameter of perforations) ratio. Dimensional analysis was carried out to find the non-dimensional parameters such as incident wave steepness, depth parameter (d/gT^2), height of structure, depth of water, wave run up (R_u/H_i), wave rundown (R_d/H_i), etc., using Buckingham's π-theorem. The experimental data collected was analyzed by plotting the graph of dimensionless wave run up and dimensionless wave rundown for various values of wave steepness and different height of structure to the depth of water. They observed that the value of R_u/H_i increases with increase in wave steepness for all values of h_s/d and d/gT^2. This was because as wave height increases there is increase in wave energy and hence run up increases with increase in wave steepness. For all values of h_s/d and d/gT^2, the dimensionless wave rundown was found to decrease with increase in wave steepness for all values of h_s/d and d/gT^2 because as wave height increases there is increase in wave energy resulting in more run up and hence less rundown. R_d/H_i was also found to increase with the increase in the depth parameter (d/gT^2) because at higher water depths, effect of curvature is more pronounced resulting in lower run up and hence more wave rundown.

Balakrishna and Hegde [8] investigated reflection coefficient (K_r) and dissipation (or loss) coefficient (K_L) for physical models of quarter circle caisson breakwater for different radii with constant S/D ratio. They observed that reflection coefficient was found to increase with wave steepness, which was similar to all earlier studies. Dissipation coefficient (K_L) decreased with increase in wave steepness. The study revealed that as wave period decreases the value of loss coefficient decreases. The study also revealed that as h_s/d increases, dissipation increases which is a reverse trend in the case of reflection, this trend is found to be true for all values of d/gT^2 values.

Generally, computational intelligence techniques viz., Artificial Neural Network (ANN), adoptive neuro fuzzy interface system, support vector machine algorithm, genetic algorithm, etc., have been efficaciously proposed as an efficient tool for modelling and predictions in coastal engineering problems [9]. In the present study, ANN and Regression (REG) approaches are used for prediction of the variables considered for evaluation of hydrodynamic performance of QBW. In ANN, Multi layer Perceptron (MLP) and Radial Basis Function (RBF) networks are adopted for training the network data. Goodness-of-Fit (GoF) test viz., Kolmogorov-Smirnov test statistic and Model Performance Analysis (MPA) viz., correlation coefficient, mean absolute error and model efficiency are applied for checking the adequacy of ANN and REG approaches to the observed (or experimental) data. This paper presents the study on evaluation of hydrodynamic performance of QBW using ANN and REG approaches with illustrative example.

Methodology

ANN modelling procedures adapt to complexity of input-output patterns and accuracy goes on increasing as more and more data become available. Figure 1 shows the architecture of ANN that consists of input layer, hidden layer, and output layer [10].

From ANN structure, it can be easily understood that input units receive data from external sources to the network and send them to the hidden units, in turn, the hidden units send and receive data only from other units in the network, and output units receive and produce data generated by the network, which goes out of the system. In this process, a typical problem is to estimate the output as a function of the input. This unknown function may be approximated by a superposition of certain activation functions such as tangent, sigmoid, polynomial, and sinusoid in ANN. A common threshold function used in ANN is the sigmoid function (f(S)) expressed by Eq. (1), which provides an output in the range of $0 \le f(S) \le 1$.

$$f(S) = \left[1 + \exp\left(-S_i\right)\right]^{-1} \text{and } S_i = \sum_{i=1}^{N} I_i W_{ij} + O_i \text{ , } and, \; j = 1, 2, 3, \ldots, M \quad (1)$$

Where, S_i is the characteristic function of i^{th} layer, I_i is the input (I) value of i^{th} layer, O_i is the output (O) value of i^{th} layer, W_{ij} is the synaptic weights between input layer (i) and hidden layer (j), N is the number of observations and M is the number of neurons (or units) of hidden layer [11].

Theoretical description of MLP network

MLP network is based on architecture with single hidden layer as shown in Figure 1. Gradient descent is the most commonly used training algorithm in MLP in which each input unit of the training data set is passed through the network from the input layer to output layer [12]. The network output is compared with the target output and output error (E) is computed using Eq. (2).

$$E = \frac{1}{2}\sum_{i=1}^{N}\left(X_i - X_i^*\right)^2 \quad (2)$$

Where, X_i is the observed value of i^{th} sample and X_i^* is the predicted value for i^{th} sample.

$$\Delta W_{ij}(M) = -\varepsilon\frac{\partial E}{\partial W_{ij}} + \alpha\Delta W_{ij}(M-1) \quad (3)$$

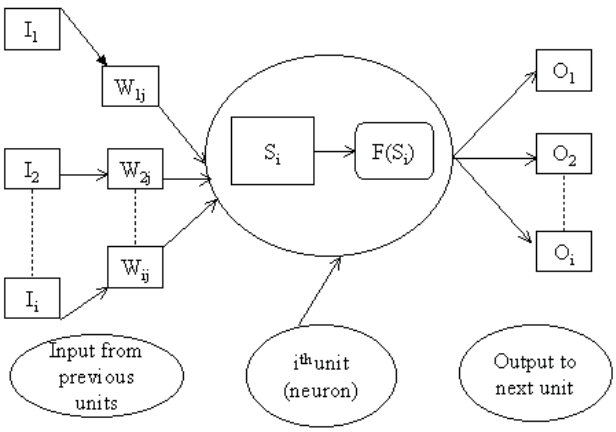

Figure 1: Architecture of ANN.

Where, $\Delta W_{ij}(M)$ is the weight increments between i^{th} and j^{th} layers during M neurons (or units) and $\Delta W_{ij}(M-1)$ is the weight increments between i^{th} and j^{th} layers during M-1 neurons (or units). In MLP, momentum factor (α) is used to speed up training in very flat region of the error surface to prevent oscillation in the weight and learning rate (ε) is used to increase the chance of avoiding the training process being trapped in local minima instead of global minima.

Theoretical description of RBF network

RBF network is supervised and three-layered feed forward neural network. The hidden layer of RBF network consists of a number of nodes and a parameter vector called a 'centre', which can be considered the weight vector. In RBF, the standard Euclidean distance is used to measure the distance of an input vector from the centre. The design of neural networks is a curve-fitting problem in a high dimensional space in RBF [11]. Training the RBF network implies finding the set of basis nodes and weights. Therefore, the learning process is to find the best fit to the training data. The transfer function of the nodes is governed by nonlinear functions that is assumed to be an approximation of the influence that data points have at the centre. The transfer function of a RBF is mostly built up of Gaussian rather than sigmoid. The Gaussian function decrease with distance from the centre. The transfer function of the nodes is governed by nonlinear functions that is assumed to be an approximation of the influence that data points have at the centre. The Euclidean length is represented by r_j that measures the radial distance between the datum vector $\underline{X}(X_1, X_2, \ldots X_M)$ and the radial centre $\underline{X}^{(j)} = (W_{1j}, W_{2j}, \ldots W_{Mj})$ can be written as:

$$r_j = \left\| \underline{X} - \underline{X}^{(j)} \right\| = \left[\sum_{i=1}^{M} \left(X_i - W_{ij} \right)^2 \right]^{1/2} \tag{4}$$

Where, $\Phi(r_j) = \Phi \| P\underline{X} - \underline{X}^{(k)} \|$ is the Euclidean norm and Φ( ) is the activation function. A suitable transfer function is then applied to r_j to give $\Phi(r_j) = \Phi \left\| \underline{X} - \underline{X}^{(k)} \right\|$. Finally, the output layer (k-1) receives a weighted linear combination of $\Phi(r_j)$.

$$X^{(k)} = W_0 + \sum_{j=1}^{N} c_j^{(k)} \Phi(r_j) = W_0 + \sum_{j=1}^{N} c_j^{(k)} \Phi\left(\left\| \underline{X} - \underline{X}^{(j)} \right\| \right) \tag{5}$$

Where c_j is the centre (c) of the neuron in the hidden layer (j) and $\Phi(r_j)$ is the response of r_j and W_0 is the bias term [13].

Theoretical description of regression approach

Number of regression models such as linear regression, auto regressive moving average and auto regressive integrated moving average are generally adopted for evaluation stationary data. In the present study, as the available data is stationary, the basic requirement to develop the regression (REG) model is satisfied and hence used for prediction of the variables. The REG models for prediction of dependant variables (K_L, K_r and K_t) using various independent variables are presented in Table 1.

In Table 1, the terms Φ_i (i=1, 2, 3…., 11) are regression coefficients and C_1, C_2 and C_3 are constants.

Goodness-of-Fit test

GoF test involving viz., Kolmogorov-Smirnov (KS) test statistic is applied for checking the adequacy of applying ANN and REG approaches to the series of observed data [14]. Theoretical description of the KS test statistic is as follows:

Sl. No.	Dependant variable	Independent variable	REG Model
1	K_L	T, H_i, H_T, H_r, K_r, K_t, H_i/d, L, H_c/H_i, H_i/gT^2, H_t/gT^2 (2)	$\Phi_1 T+\Phi_2 H_i+\Phi_3 H_T+\Phi_4 H_r+\Phi_5 K_r+\Phi_6 K_t+\Phi_7 H_i/d+\Phi_8 L+\Phi_9 H_c/H_i+\Phi_{10} H_i/gT^2+\Phi_{11} H_t/gT^2(2)+C_1$
2	K_r	T, H_i, H_T, H_r, K_L, K_t, H_i/d, L, H_c/H_i, H_i/gT^2, H_t/gT^2 (2)	$\Phi_1 T+\Phi_2 H_i+\Phi_3 H_T+\Phi_4 H_r+\Phi_5 K_L+\Phi_6 K_t+\Phi_7 H_i/d+\Phi_8 L+\Phi_9 H_c/H_i+\Phi_{10} H_i/gT^2+\Phi_{11} H_t/gT^2(2)+C_2$
3	K_t	T, H_i, H_T, H_r, K_L, K_r, H_i/d, L, H_c/H_i, H_i/gT^2, H_t/gT^2 (2)	$\Phi_1 T+\Phi_2 H_i+\Phi_3 H_T+\Phi_4 H_r+\Phi_5 K_L+\Phi_6 K_r+\Phi_7 H_i/d+\Phi_8 L+\Phi_9 H_c/H_i+\Phi_{10} H_i/gT^2+\Phi_{11} H_t/gT^2(2)+C_3$

Table 1: Description of REG Model.

$$KS_C = \underset{i=1}{\overset{N}{Max}} \left(F_e(X_i) - F_D(X_i) \right) \tag{6}$$

Where, $F_e(X_i)=(i-0.35)/N$ is the empirical Cumulative Distribution Function (CDF) of X_i and $F_D(X_i)$ is the computed CDF of X_i by ANN and REG approaches.

Model performance analysis

The performance of ANN and REG approaches adopted in prediction of the variables (K_L, K_t and K_r) is evaluated by Model Performance Indicators (MPIs) viz., Correlation Coefficient (CC), Mean Absolute Error (MAE) and Model Efficiency (MEF), and are given below:

$$\left.\begin{aligned} CC &= \frac{\sum_{i=1}^{N} \left(X_i - \overline{X} \right) \left(X_i^* - \overline{X^*} \right)}{\sqrt{\left(\sum_{i=1}^{N} \left(X_i - \overline{X} \right)^2 \right) \left(\sum_{i=1}^{N} \left(X_i^* - \overline{X^*} \right)^2 \right)}} \\ MAE(\%) &= \left(\frac{1}{N} \sum_{i=1}^{N} \left| X_i - X_i^* \right| \right) * 100 \\ MEF(\%) &= \left(1 - \frac{\sum_{i=1}^{N} \left(X_i - X_i^* \right)^2}{\sum_{i=1}^{N} \left(X_i - \overline{X} \right)^2} \right) * 100 \end{aligned}\right\} \tag{7}$$

Where, $\overline{X^*}$ is the average value of observed (or experimental) data and $\overline{X^*}$ is the average value of predicted data [15]. The model with high CC, less MAE and better MEF is considered as best suited amongst ANN and REG approaches adopted in prediction of the variables used for evaluation of hydrodynamic performance of QBW.

Application

In this paper, a study on comparison of hydrodynamic performance of QBW was carried out. The experimental data viz., depth of water (d), wave period (T), incident wave height (H_i), transmitted wave height (H_t), reflected wave height (H_r), transmission coefficient (K_t), loss coefficient (K_L), wave length (L), reflection coefficient (K_r), incident wave steepness (H_i/gT^2), relative freeboard (h_c/H_i) and relative wave height (H_i/d) collected at National Institute of Technology, Surathkal, is analysed by plotting the non-dimensional graphs of reflection coefficient, reflected wave height and incident wave height for various values of wave steepness. The values were used for prediction of QBW adopting ANN and REG approaches.

Description of experimental setup

The study was conducted in the regular wave flume available in the

marine structures laboratory of the Department of Applied Mechanics and Hydraulics, National Institute of Technology Karnataka, Surathkal. The experiments were performed in wave flume with dimensions of 50 m long, 0.74 m wide and 1.1 m deep. Out of 50 m, 42 m length has smooth concrete bed. It has a 6.3 m long, 1.5 m wide and 1.4 m deep chamber at one end, where, wave flap is hinged at the bottom generates waves. The flap is controlled by an induction motor of 11 kw, 1450 rpm and is regulated by an inverter drive, 0 to 50 Hz rotating with a speed range of, 0 to 1550 rpm. This facility is able to generate regular waves of 0.08 to 0.24 m of periods 0.8 to 4 sec.

A series of vertical asbestos sheets are spaced at about 10 cm distance from each other and kept parallel to the length of the flume to dissipate the generated waves by damping the disturbance caused by successive reflection and to smoothen them. The QBW model is placed in the flume 28 m away from the wave flap, above the rubble mound foundation (Figure 2). The slope used for the rubble foundation is 1:2. Three capacitance type wave probes were used for measuring the incident and reflected wave heights. The wave probes were placed at a distance of 4 m from the centre of the model.

Results and Discussions

The determined optimum network architecture with model parameters obtained from MLP and RBF networks, and regression models was used for prediction of QBW. In ANN (using MLP and RBF networks), 75% of data was used for training (TRG) and 25% of data used for testing (TES) the experimental data. Similarly, in REG, 75% of data was used for calibration (CAL) and 25% of data used for validation (VAL) while developing the REG equations. Statistical software, namely, SPSS (Statistical Package for the Social Sciences) is used to predict the hydrodynamic characteristics viz., K_L, K_r and K_t of QBW using ANN and REG approaches. The experimental data was trained with MLP and RBF networks to determine the Optimum Network Architecture (ONA) for the variables viz., K_L, K_r and K_t. The determined ONAs with model parameters obtained from MLP and RBF networks, and REG equations were used for prediction of QBW. The results obtained from ANN (using MLP and RBF networks) and REG approaches were presented in the following sections.

Prediction of K_L, K_r and K_t using MLP

The momentum factor (α) and learning rate (ε) were fixed as 0.6 and 0.05 while optimizing the network architecture of MLP for K_L, K_r and K_t. The network data was trained with ONA (i.e., 11-21-1) with one input layer with 11 units, one hidden layer with 21 hidden units and one output layer with one unit. The network was tested with model parameters for prediction of the variables (K_L, K_r and K_t) to evaluate the hydrodynamic performance of QBW.

Prediction of K_L, K_r and K_t using RBF

By using the procedures of RBF, as described earlier, the experimental data was trained with model parameters to determine the ONAs of K_L, K_r and K_t. The ONAs were determined as 12-7-1 for K_L whereas 12-10-1 for K_r and 12-4-1 for K_t. The ONAs were further used to test the network data of the variables viz., K_L, K_r and K_t.

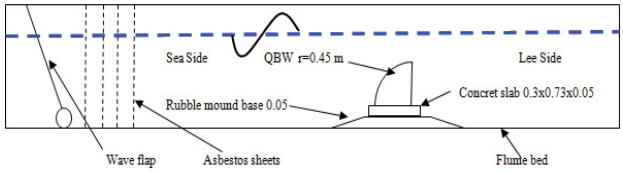

Figure 2: A schematic diagram of experimental setup.

Prediction of K_L, K_r and K_t using REG

By using the procedures of REG approach, as described earlier, the REG equations for the dependant variable (s) in terms of the independent variables were developed and given as:

$$K_L=(-0.625)T+(-0.022)H_i+(0.021)H_T+(0.031)H_r+(-0.690)K_r+(-1.829)K_t+(0.153)H_i/d+ (0.266)L+(0.011)H_c/H_i+(-0.022)H_i/gT^2+(0.016)H_i/gT^2 (2)+2.291$$

$$K_r=(-0.396)T+(-0.007)H_i+(0.001)H_T+(0.062)H_r+(-0.469)K_L+(-0.767)K_t+(-0.275)H_i/d+(0.196)L+(-0.002)H_c/H_i+(0.009)H_i/gT^2+(0.081)H_i/gT^2 (2) +1.070$$

$$K_t=(-0.185)T+(-0.028)H_i+(0.025)H_T+(0.011)H_r+(-0.431)K_L+(-0.266)K_r+(0.393)H_i/d+(0.076)L+(0.008)H_c/H_i+(0.104)H_i/gT^2+(0.104)H_i/gT^2 (2) +1.120$$

Analysis based on GoF test

The KS test statistic values of ANN (using MLP and RBF networks) and REG approaches for the variables K_L, K_r and K_t were computed and found to be varied between 0.125 and 0.210. These values were noted to be less than of its theoretical value of 0.221 at 5% level, and at this level, both ANN and REG approaches are found to be acceptable for prediction of the desired variables (K_L, K_r and K_t). The predicted variables were used for evaluation of hydrodynamic performance of QBW.

Performance analysis based on MPIs

The model performance of ANN and REG approaches used in prediction of the variables (K_L, K_r and K_t) was evaluated by MPIs and the results are presented in Tables 2 and 3.

From Table 2, it could be noticed that the MEF obtained from MLP is relatively higher when compared with the corresponding values of RBF and REG. Also, from Table 2, it could be noticed that the percentage of MAE obtained from MLP is less than the corresponding values of RBF and REG. From Table 3, it may be noted that the CC values obtained from MLP for the predicted variables vary between 0.950 and 0.998. The time series plots of predicted values of the variables (K_L, K_r and K_t) using MLP and REG together with observed data are presented in Figures 3 to 5. The scatter plots of observed and predicted values of the variables with model fit and R^2 (coefficient of determination) values are presented in Figures 6 to 8.

Variables	Computed values of MEF and MAE											
	MEF (%)						MAE (%)					
	MLP		RBF		REG		MLP		RBF		REG	
	TRG	TES	TRG	TES	CAL	VAL	TRG	TES	TRG	TES	CAL	VAL
K_L	96.3	98.8	58.8	89.9	92.6	95.8	1.6	1.2	6.8	3.5	2.6	2.3
K_r	90.9	97.7	71.7	78.7	92.0	94.6	1.6	0.9	3.0	2.7	1.7	1.5
K_t	97.3	99.5	66.7	86.2	96.5	96.7	0.9	0.5	3.7	2.7	1.2	1.5

Table 2: Values of MPIs for K_L, K_r and K_t given by MLP, RBF and REG.

Variables	Computed values of CC					
	MLP		RBF		REG	
	TRG	TES	TRG	TES	CAL	VAL
K_L	0.981	0.994	0.769	0.956	0.962	0.980
K_r	0.950	0.968	0.836	0.677	0.956	0.945
K_t	0.986	0.998	0.825	0.959	0.982	0.983

Table 3: Values of CC for K_L, K_r and K_t given by MLP, RBF and REG.

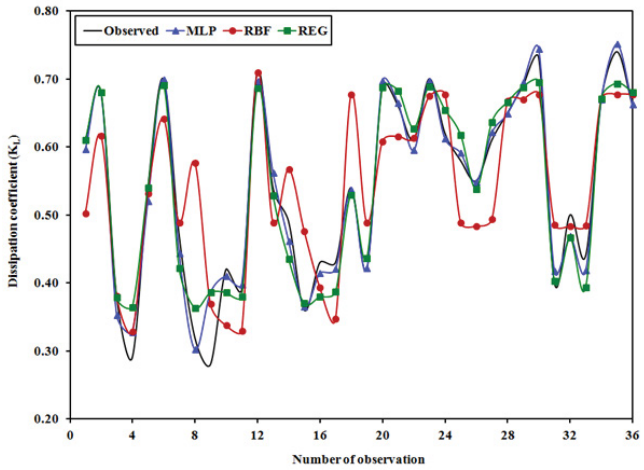

Figure 3: Time series plots of observed and predicted values of K_L.

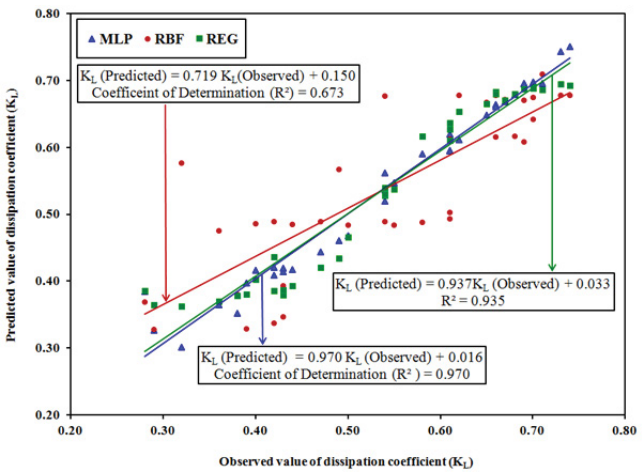

Figure 6: Scatter plots of observed and predicted values of K_L.

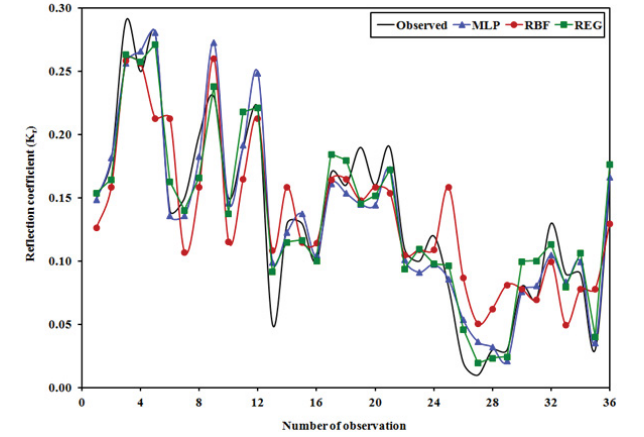

Figure 4: Time series plots of observed and predicted values of K_r.

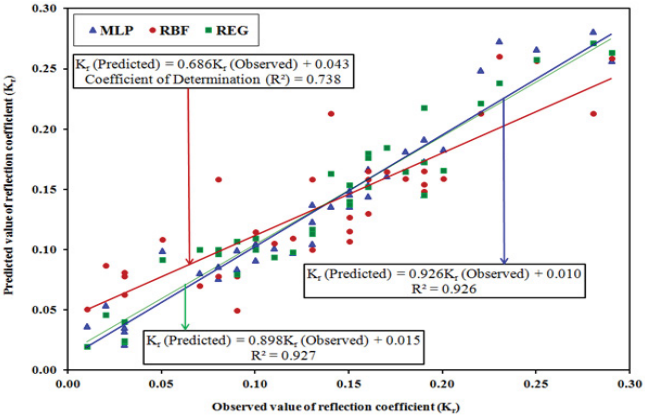

Figure 7: Scatter plots of observed and predicted values of K_r.

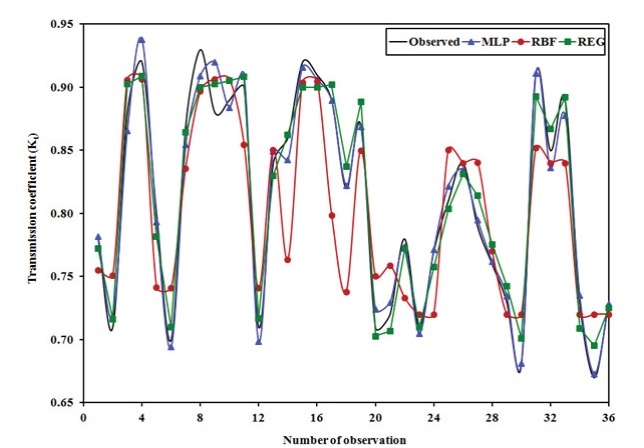

Figure 5: Time series plots of observed and predicted values of K_t.

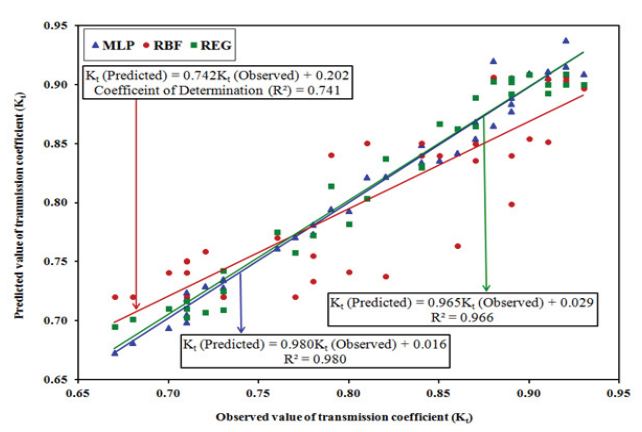

Figure 8: Scatter plots of observed and predicted values of K_t.

From Figures 3 to 5, it can be seen that the predicted values of the variables (K_L, K_r and K_t) using MLP network gives better performance than RBF and REG during testing period. From Figures 6 to 8, it can be seen that the R^2 values obtained from fitted model using MLP for K_L, K_r and K_t variables are 0.970, 0.926 and 0.980, which indicates that there is a perfect fit between the observed and predicted variables.

Analysis based on descriptive statistics

In addition to MPIs, the performance of ANN (using MLP and RBF) and REG approaches adopted in prediction of the variables (K_L,

Descriptive statistics	Observed		MLP		RBF		REG	
	Data points (1 to 27)	Data points (28 to 36)	TRG	TES	TRG	TES	CAL	VAL
Dissipation (or loss) coefficient (K_L)								
Average	0.519	0.609	0.516	0.608	0.515	0.611	0.522	0.596
SD	0.134	0.128	0.129	0.135	0.119	0.095	0.129	0.133
CV (%)	25.8	21.0	25.0	22.2	23.0	15.5	24.8	22.2
C_S	-0.205	-0.789	-0.033	-0.651	-0.113	-0.852	0.068	-0.918
C_K	-1.139	-1.112	-1.386	-1.501	-1.108	-1.714	-1.760	-1.381
Reflection coefficient (K_r)								
Average	0.154	0.079	0.151	0.078	0.154	0.081	0.153	0.085
SD	0.070	0.046	0.066	0.045	0.054	0.023	0.064	0.050
CV (%)	45.3	57.9	43.7	57.7	34.9	28.4	41.9	58.1
C_S	-0.110	0.537	0.491	0.666	0.535	1.166	0.138	0.349
C_K	0.049	-0.430	-0.297	0.693	-0.104	2.177	-0.284	0.017
Transmission coefficient (K_t)								
Average	0.823	0.771	0.821	0.770	0.814	0.767	0.823	0.778
SD	0.076	0.089	0.076	0.085	0.070	0.060	0.077	0.083
CV (%)	9.3	11.5	9.3	11.0	8.6	7.8	9.4	10.7
C_S	-0.329	0.602	-0.287	0.635	0.100	0.649	-0.355	0.608
C_K	-1.249	-1.238	-1.154	-0.949	-1.663	-1.836	-1.438	-1.687

Table 4: Descriptive statistics of predicated variables (K_L, K_r and K_t) by MLP, RBF and REG.

K_r and K_t) was analyzed through the descriptive statistics (i.e., Average, Standard Deviation (SD), Coefficient of Variation (CV), Coefficient of Skewness (C_S) and Coefficient of Kurtosis (C_K)) and the results are presented in Table 4. Based on the GoF test results using KS test statistic and MPA using MPIs, the study suggested that MLP is better suited amongst MLP, RBF and REG models adopted for prediction of the variables viz., K_L, K_r and K_t, which are used for evaluation of hydrodynamic performance of QBW.

By using the values of the descriptive statistics of the K_L, as given in Table 4, the percentage of variation on the average of predicted value using MLP for K_L, with reference to average of observed value, is computed as 0.6% and 0.2% during TRG and TES respectively. For K_r, the values obtained from MLP during TRG and TES are found to be 1.9% and 1.3% respectively. Likewise, for K_t, it may be noted that the percentage of variation on the average of predicted value using MLP, with reference to average of observed value is computed as 0.2% and 0.1% during training and testing.

Conclusions

The paper described the procedures involved in prediction of the variables viz., K_L, K_r and K_t adopting ANN (using MLP and RBF) and REG approaches. These variables were used for evaluation of hydrodynamic performance of QBW. From the results of data analysis, the following conclusions were drawn from the study:

1) Optimum MLP network architecture viz., 11-21-1 was used for training the network. The ONA of MLP with model parameters was used for testing the network data and prediction of variables

2) Regression equations developed through REG approach was used for prediction of the variables.

3) KS test results supported the use of ANN and REG approaches used in determining the hydrodynamic characteristics parameters.

4) GoF test results using KS test statistic and MPA using MPIs confirmed that the MLP is better suited amongst MLP, RBF and REG models adopted for prediction of the variables viz., K_L, K_r and K_t.

5) The percentage of MAE obtained from MLP is less than the corresponding values of RBF and REG during training (or calibration) and testing (or validation) for all three predicted variables. While testing the network (i.e, experimental) data, the MAE using MLP for the predicted variables K_L, K_r and K_t were computed as 1.2%, 0.9% and 0.5% respectively.

6) For K_L, the values of CC and MEF given by MLP were computed as 0.994 and 98.8% respectively during testing period. Similarly, the values of CC and MEF were computed as 0.968 and 97.7% for K_r whereas 0.998 and 99.5% for K_t.

7) The percentage of variation on the average of predicted value using MLP, with reference to average of observed value, was computed as 0.2% for K_L, 1.3% for K_r and 0.1% for K_t while testing the network data.

Acknowledgements

The author is grateful to Dr. (Mrs.) V.V. Bhosekar, Additional Director and Director In-charge, Central Water and Power Research Station, Pune, for providing research facilities to carry out the study. The author is thankful to Shri N. Ramesh, Research Scholar, National Institute of Technology, Surathkal, for the supply of experimental data used in the study.

References

1. Xie SL, Li YB, Wu YQ, Gu HB (2006) Preliminary research on wave forces on quarter circular breakwater. Ocean Engineering 24: 14-18.
2. Jiang XL, Gu HB, Li YB (2008) Numerical simulation on hydraulic performances of quarter circular breakwater. China Ocean Engineering 22: 585-594.
3. Shi YJ, Wu, Mi-Ling, Jiang XL, Li, et al. (2011) Experimental research on reflection and transmitting performance of Quarter circle Breakwater under regular and irregular waves. China Ocean Engineering 25: 469-478.
4. Shao LM (2003) Separation of incident waves and reflected waves and study of reflection coefficient. Dalian University of Technology, Dalian.
5. Hegde AV, Ravikiran L (2013) Wave structure interaction for submerged quarter circle breakwaters of different radii-reflection characteristics. World Academy of Science, Engineering and Technology 7: 1367-1371.
6. Hafeeda V, Binumol S, Hegde AV, Subba R (2014) Wave reflection by emerged sea side perforated quarter circle breakwater. Int J Earth Sci Engg 7: 454-460.
7. Binumol S, Subba R, Hegde AV (2015) Runup and rundown characteristics of an emerged seaside perforated quarter circle breakwater. Aquatic Pocedia 4: 234-239.
8. Balakrishna K, Hegde AV (2015) Reflection and dissipation characteristics of non-overtopping quarter circle breakwater with low-mound rubble base. J Adv Res Ocean Engg 1: 44-054.
9. Amr HE, El-Shafie A, Hasan GE, Shehata A, Taha MR (2011) Artificial neural network technique for rainfall forecasting applied to Alexandria, Egypt. Int J Phys Sci 6: 1306-1316.
10. Tokar S, Markus M (2000) Precipitation runoff modelling using artificial neural network and conceptual models. J Hydrologic Engg 5: 156-161.
11. Kaltech M (2008) Rainfall-runoff modelling using artificial neural networks: modelling and understanding. J Environmental Sci 6: 53-58.
12. Deshpandey RR (2012) On the rainfall time series prediction using multilayer perceptron artificial neural network. Int J Emerging Technol and Adv Engg 2: 2250-2459.
13. Karthik S, Subba Rao (2017) Application of soft computing in breakwater studies – A Review. Int J Innovative Res Sci, Engg Technol 6: 8355-8359.
14. D'Agostino BR, Stephens AM (1986) Goodness-of-Fit Techniques. M/s Marcel Dekkar Inc., New York.
15. Chen J, Adams BJ (2006) Integration of artificial neural networks with conceptual models in rainfall-runoff modeling. J Hydrology 318: 232-249.